Australian Meteorological and Oceanographic Journal 60 (2010) 25-36

Darwin's mid-evening surge

Gerald L. Thomsen and Roger K. Smith
Meteorological Institute, University of Munich, Germany

(Manuscript received October 2008, revised December 2009)

The passage of a sea-breeze front is a regular occurrence in Darwin, Northern Territory, Australia. On some days, what has been christened a 'second sea-breeze' is observed during the evening, an occurrence that has puzzled forecasters. We investigate this phenomenon using high-resolution numerical simulations of selected events. The simulations are compared with available data from automatic weather stations. They show that, on occasions when a 'second sea-breeze' is observed, the prevailing easterly to southeasterly winds over the 'Top End' advect a band of dry inland air northwestwards towards the Tiwi Islands during the morning. This dry air subsequently moves southwestwards towards Darwin and as it passes in the late evening, it is replaced by moist maritime air. Since this replacement is not a real sea-breeze, we refer to the phenomenon as a mid-evening surge. The results of idealised model calculations support these findings.

Introduction

The passage of the sea-breeze front can be a great relief when it is very hot as the temperature may fall by several degrees and typically the wind speed increases. However, the arrival of the sea-breeze air brings an increase in humidity. Whether a particular location is reached by a sea-breeze depends on a number of factors including the distance to the coast, the broadscale wind field and the surface-temperature difference between land and sea. The latter, in turn, depends on the insolation, on the local albedo, and on the soil moisture. During the dry season, Darwin frequently experiences what appear to be two distinct sea-breezes. The first sea-breeze front passes around midday and the onset of what has been interpreted as the second sea-breeze occurs in the late evening. The 'second sea-breeze' has been thought by forecasters to be caused by the small-scale shape of the coastline around Darwin. The results presented herein suggest that the name 'second sea-breeze' is a misleading description of the phenomenon, because the moisture increase that accompanies it is associated with the advection of maritime air by the broadscale wind field rather than by a local wind circulation driven by the temperature difference between land and sea. Nevertheless its passage is accompanied also by an increase in wind speed and a change in wind direction and for this reason we refer to the phenomenon here as a mid-evening surge.

Corresponding author address: Dr Gerald Thomsen, Meteorologisches Institut, Theresienstr. 37, 80333 München, Germany.
Email: gerald@meteo.physik.uni-muenchen.de

To investigate the regular sea-breeze and the mid-evening surge we performed high-resolution numerical simulations of six events that occurred in late 2006. Here we present calculations for two of these cases and compare them with available data from the automatic weather station (AWS) at Darwin Airport. We examine also a null event in support of the interpretations we present in the following sections. Finally we present two idealised calculations that serve to isolate the essential features of the mid-evening surge.

Model setup

The numerical model used for the study is the Pennsylvania State University/National Center for Atmospheric Research mesoscale model (MM5). A detailed description of the model can be found in Grell et al. (1995). The model is configured with 23 σ-levels that provide a relatively high resolution in the boundary layer. The seventeen levels below 4 km are centred at heights of approximately: 18, 54, 109, 182, 257, 332, 445, 599, 754, 994, 1322, 1662, 2016, 2383, 2767, 3168 and 3588 m.

The calculations are carried out on the two horizontal domains shown in Fig. 1(a). The outer domain has 221 × 221 grid-points with a horizontal grid size of 9 km and the inner domain has 301 × 301 points with a grid size of 3 km. The terrain land use and topography are taken from the United States Geological Survey data-set implemented in MM5 and have a 5′ resolution in the outer domain and 2′ resolution in the inner domain. The time step is chosen as 27 s for the outer domain and 9 s for the inner domain. The terrain elevation around Darwin is shown in Fig. 1(b).

Fig. 1 Left panel: terrain elevation in the large MM5 domain. The dashed box indicates the position of the high-resolution nest. Right panel: terrain elevation in the high-resolution MM5 nest around Darwin. The coastline is shown as derived from the MM5 terrain elevation.

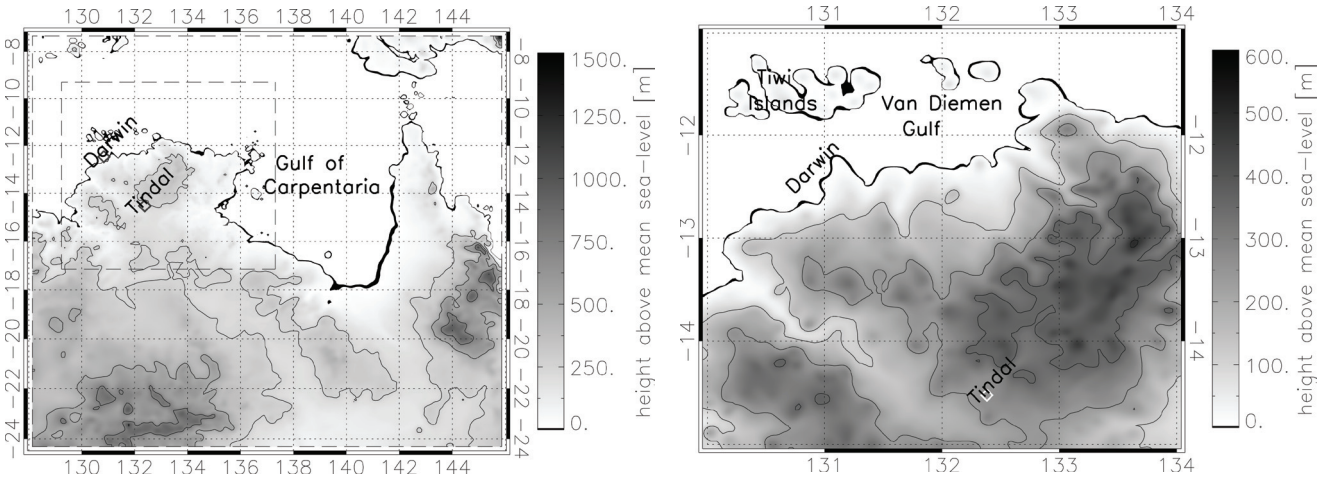

Analysis data from the European Centre for Medium Range Weather Forecasts (ECMWF) with a horizontal resolution of 0.25° are used to provide initial and boundary conditions (including surface and sea-surface temperatures) for the calculations. A bucket model is used to account for soil moisture. The model is initialised with the soil moisture values used by Thomsen and Smith (2006), which are significantly lower than those in the ECMWF analyses. Thomsen (2006) found that the ECMWF values were much too moist for the north Australian dry season. The short and long-wave cloud and ground radiation scheme takes into account diurnal variations. The Grell scheme (Grell 1993) is used to parametrise deep cumulus convection and the Dudhia scheme as a parametrisation for cloud microphysical processes (Dudhia 1989).

The MRF scheme (Hong and Pan 1996) is used for the parametrisation of the planetary boundary layer. A sensitivity study of the different boundary-layer parametrisations available in MM5 was carried out by Thomsen and Smith (2008). That study focussed on case studies of sea-breeze convergence lines in the north Australian region and it was shown that the model performed best when the MRF scheme was used. In the present study, the surface (2 m) water vapour mixing ratio is of fundamental importance for assessing the passage of a sea-breeze. However, we discovered that the calculation of this quantity in the MRF and other schemes is not continuous in time and space, since different formulae are applied for different boundary-layer stability states. The resulting jumps in the moisture field are misleading for the identification of sea-breeze passages and it proved necessary to modify the MRF scheme to extrapolate the 2 m moisture from the lowest model layer, independently of the boundary-layer stability.

Selected events

The Bureau of Meteorology Regional Forecasting Centre in Darwin provided data for the period October to December 2006 and reported seventeen mid-evening surge events which occurred in Darwin within this time period (those of 8, 9, 14, 15, 16, 17, 23 October, 1, 18, 20, 21, 22, 23, 24, 27 November and 14, 20 December). We performed simulations for six of these (those of 8, 9, 14, 15, 23 October and 23 November) plus a null event, a day on which there was no mid-evening surge (5 November). For reasons of space we describe only two of these simulations in detail, those of 8 October and 14 October. These two cases are typical of the other four. In addition to these real cases, we performed two idealised experiments in support of our explanation for the occurrence of the mid-evening surge. Herein, all times are given in Australian Central Standard Time (CST) which is 9.5 h ahead of Coordinated Universal Time (UTC).

8 October 2006

Figure 2 compares observed time series of the 2 m water vapour mixing ratio and temperature and the 10 m wind speed and direction (averaged over 10 minutes) from the AWS station[1] at Darwin Airport with similar data obtained from the nearest model grid cell, a 3 × 3 km square. The blue curves are for a model run initialised at 0000 UTC 7 October, referred to as R07, and the red curves for a run initialised 24 hours later, referred to as R08. Before commenting on this figure in detail it should be noted that a comparison of fields at a model grid-point adjacent to the coast with that at a

1 The AWS is on a well exposed site and is located about 6 km from the coast to the west and 9 km from the coast to the north.

Fig. 2 Comparison of time series of AWS data at Darwin on 8 and 9 October with model predictions: (a) 2 m water vapour mixing ratio, (b) 10-minute averaged 10 m wind direction, (c) 2 m temperature and (d) 10-minute averaged 10 m wind speed. Black lines correspond to the observations and blue and red lines correspond to the model results, where the model was initialised at 0930 CST on 7 October and on 8 October, respectively. The Roman numbers correspond to events described in the text.

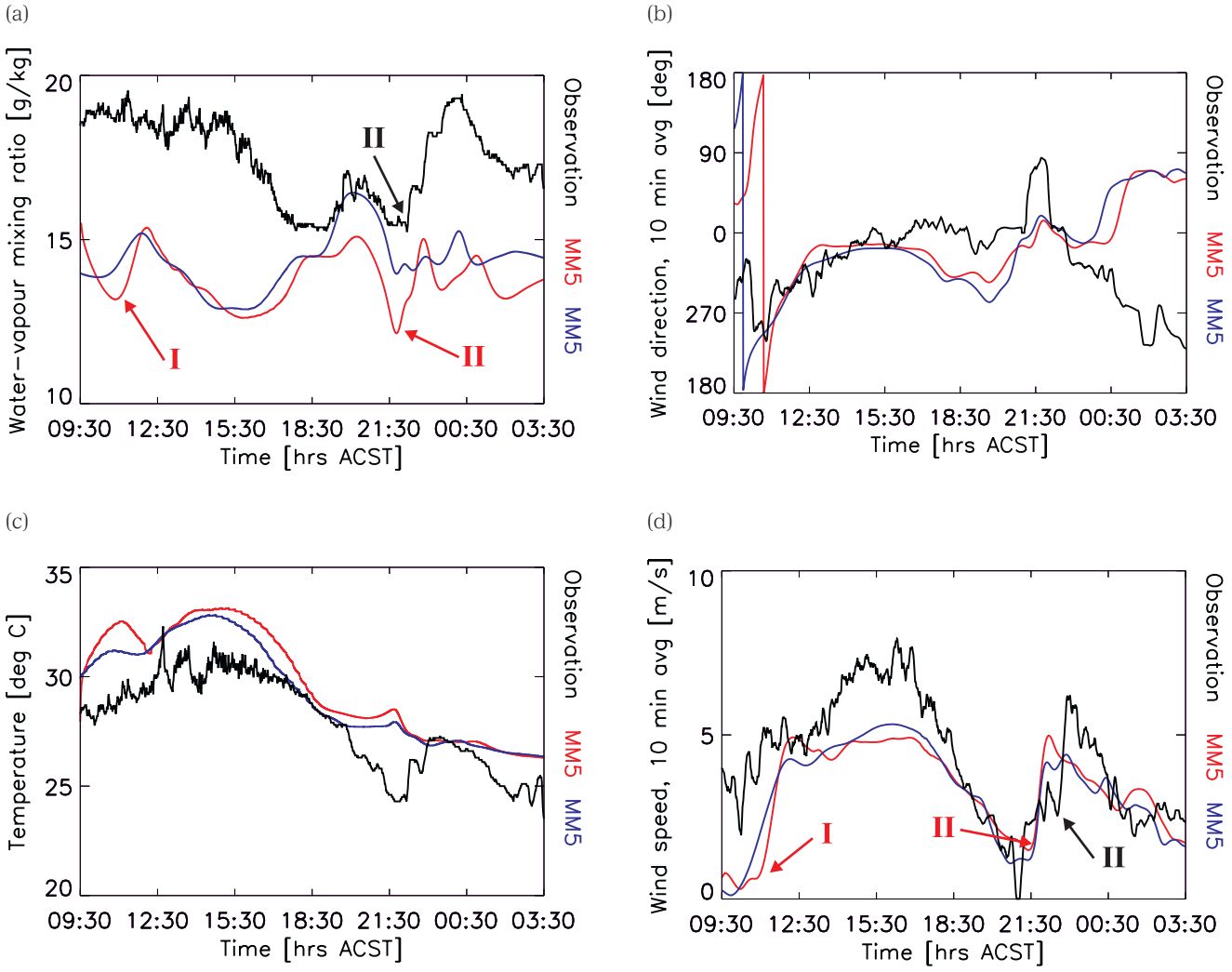

single station is a very stringent test of the model. With this in mind, it is not surprising that some aspects of the comparison are moderately good, while others might be judged as poor. This situation is probably as much a reflection of the state-of-the-art of mesoscale analysis and modelling in the tropics as it is the stringency of the test that we are using. First, the near-surface air in the model is clearly too dry, the water vapour mixing ratio being up to 5 g/kg less than that observed (Fig. 2(a)). This dryness is seen in both forecasts and is clearly an error in the ECMWF analyses. A calculation with soil moisture values as high as in the ECMWF data-set showed that the air is still drier than observed, but the timing of the sea-breeze front is worse than in the calculation with the drier surface. In fact, an examination of the ECMWF analysis at 0000 UTC 8 October showed that a change in wind direction from northeasterly to westerly occurs too far south in the ECMWF analysis, leaving the Darwin region in northeasterly winds although westerlies were observed. Of course, these northeasterly winds are much drier than the observed westerlies, which explains the discrepancy between model and observations. Interestingly, MM5 reproduces this wind change too far south in R07 as well.

The model shows three periods with a sharp increase in moisture. The first of them at 1100 CST (marked I in Fig. 2) corresponds to a normal sea-breeze onset. It is accompanied by a small decline in temperature in the order of 1 K (panel (c)), a steady veering of the wind direction from one with an easterly component at 0930 CST to a westerly at 1100 CST (panel (b)), and a marked freshening of the wind during this time (panel (d)). This feature is not seen in the observations as the winds were already westerly at 0930 CST (and indeed for the previous six hours (not shown)). After the passage

Fig. 3 Water vapour mixing ratio at 2 m (shaded) and horizontal wind vectors on the σ = 0.955 surface at (a) 1000 CST, (b) 1400 CST, (c) 1600 CST, (d) 1800 CST, (e) 2200 CST on 8 October and (f) 0200 CST on 9 October. The model run shown here was initialised on 8 October at 0930 CST, corresponding to the red lines in Fig. 2. The location of Darwin is indicated in all panels. The area shown in panels (b-f) is indicated by the box in panel (a). The line in panel (e) indicates the position of the cross section shown in Fig. 12.

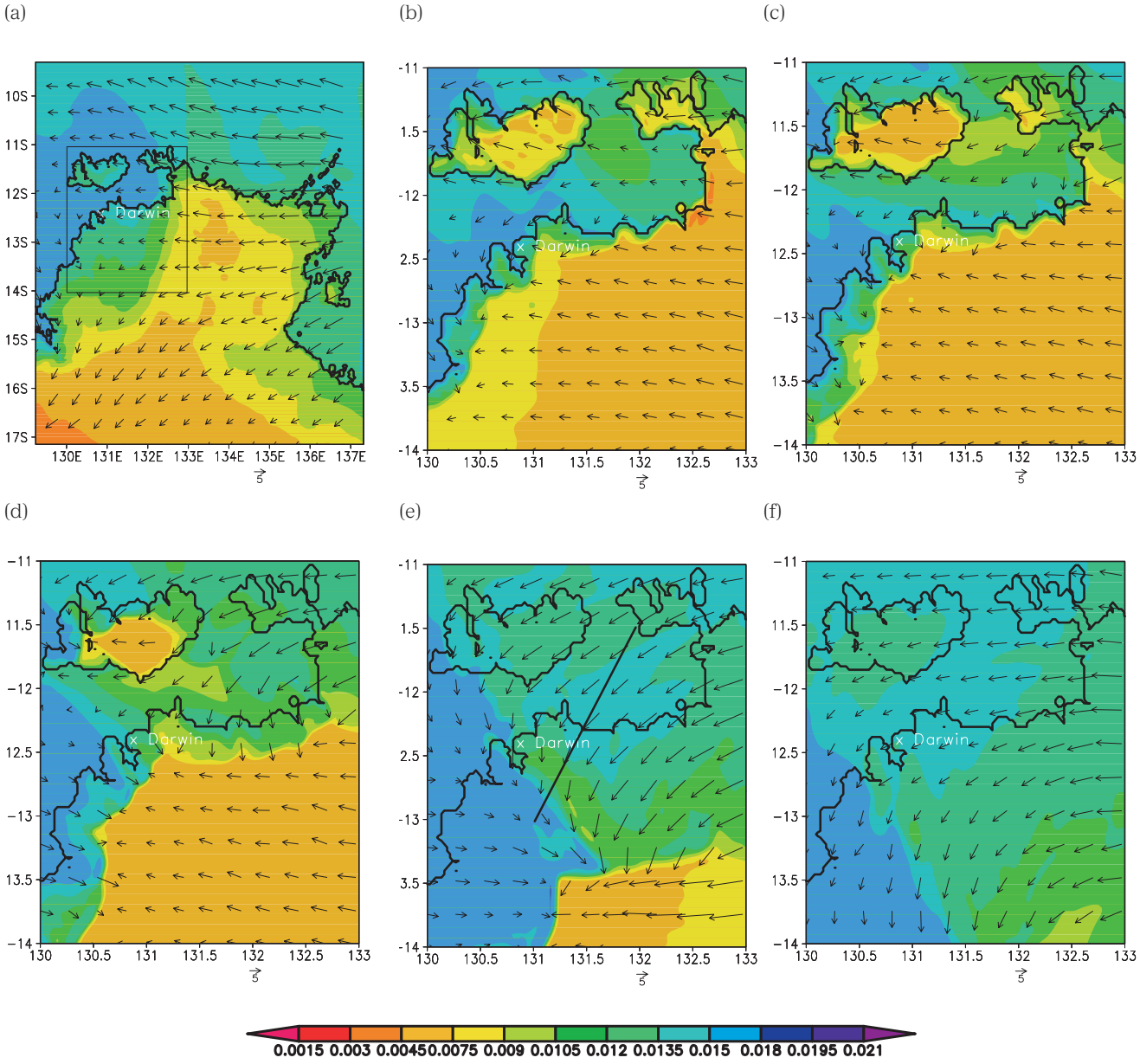

of the sea-breeze in the model, the wind direction agrees well with that in the observations until late afternoon, but the wind speed is underestimated by up to 2.5 m s^{-1}. In the model and in the observations, the northerly winds persist for much of the afternoon (panel (b)). From about 1430 CST onwards, the moisture and temperature fall steadily. The model temperature is mostly a few degrees warmer than observed. The observations show a relatively dry period from about 1700 CST until 1900 CST, which occurs earlier in the model, between 1230 CST and 1700 CST. In both the model and observations, the moisture increase that marks the end of this dry period is accompanied by a steady change in wind direction from a northerly to a northwesterly and with a steady decline in wind speed, although the wind direction change is smaller in the model. The observed moistening of approximately 2 g/kg was captured well by R07, but less well by R08. The observations show a short time period around 2100 CST with reduced moisture and with easterly winds after which the wind backs to northerly and at about 2200 CST to northwesterly, accompanied by a sharp increase in wind speed. The increase in wind speed is followed by a further period of moistening.

It is these features (marked II in Fig. 2) that are normally interpreted as the 'second sea-breeze', or what we call the mid-evening surge. The model captures these features reasonably well with a timing error of no more than half an hour. In contrast to the earlier moisture increase, the observed moistening was captured better by R08. The change in wind speed and direction accompanying the passage of the mid-evening surge coincides with the passage of a convergence zone between two different air masses which we describe in more detail in a later section. The observed temperature falls several degrees after sunset, which occurs a little after 1900 CST, while that in the model remains more or less constant. This discrepancy is most likely attributable to the inability of the model to capture the shallow radiation inversion that forms over the land during a period of light winds. Such inversions are rapidly destroyed by a freshening of the winds (see e.g. Smith et al. (1995); Thomsen et al. (2009)). After midnight, the observations show renewed cooling, while the model does not. The decoupling of the near-surface air resulting from this cooling offers a plausible explanation for the deviation between the wind direction in the model and observations after this time.

We examine now the course of events that led to the mid-evening surge. Figure 3 shows the model wind field on the σ = 0.955 surface (approximately 330 m above mean sea-level) and the 2 m water vapour mixing ratio at different times on 8 and 9 October 2006. Panel (a) shows the situation at 1000 CST, just half an hour after model initialisation. A region of relatively dry air extends far north into the eastern half of the Top End. Panel (b) shows the situation at 1400 CST in the area indicated by the box in panel (a). The air over the land has dried significantly compared with the maritime air due to strong vertical mixing. The northern part of the Top End lies in the easterlies and these winds have advected some of the dry air over the Van Diemen Gulf, establishing a wedge of dry air between the Tiwi Islands and the continent. By 1600 CST (panel (c)), the continued advection of dry air has broadened this wedge and the easterly winds have pushed the dry air just to the east of Darwin. The further westward movement of this air is prevented by the development of the sea-breeze, which becomes sufficiently strong to oppose the background easterly flow. In contrast, to the northeast of Darwin, the orientation of the coastline is more east-west and the background easterly wind field is able to advect the dry air over the Van-Diemen Gulf. By 1800 CST (panel (d)) the sea-breeze has intensified and the dry air that had been advected westwards into the Darwin area has retreated inland, but the dry air wedge has drifted southwestwards and has begun to affect Darwin. By 2200 CST (panel (e)) the centre of the dry air has reached Darwin and the moisture minimum has been reached. By 0200 CST (panel (f)) the wedge has passed over Darwin and has been replaced again by moist air, the onset of which corresponds with that of the mid-evening surge.

Figure 4 shows a visible satellite image at 1603 CST on 8 October. The positions of the sea-breeze fronts are located presumably close to the edge of the cumulus cloud field

Fig. 4 Meteosat visible image at 1603 CST, 8 October 2006: the ellipse indicates a band of dry air.

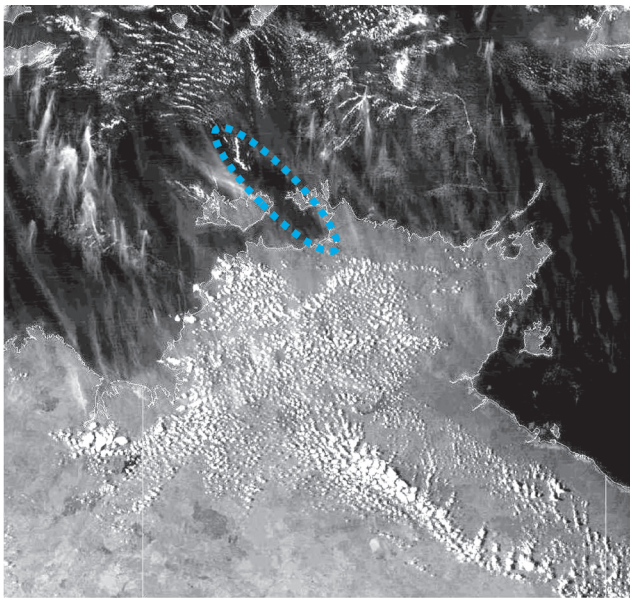

centred over the land. This cloud field is shifted to the west by the generally easterly wind regime. The near-surface air in the cloudy area is relatively dry while the air behind sea-breeze fronts is moister. The band of dry air is indicated by a dashed ellipse, where there is little indication of shallow convection. The dry air in the model has been advected approximately 25 km too far to the southwest at 1600 CST (not shown here).

14 October 2006

The key difference between this event and the 8 October event, as well as the other events simulated, is the absence of the late-afternoon moisture increase in the model.

Figure 5 shows time series of the 2 m water vapour mixing ratio, temperature and dew-point and the 10 m wind speed and direction (averaged over 10 minutes) at Darwin. The modelled 2 m water vapour mixing ratio has two periods of maximum increase at approximately 1230 CST and 2200 CST. The first peak corresponds to the regular sea-breeze (marked I) and is about 30 minutes earlier than that observed. The wind direction changed from easterly to westerly with the passage of the sea-breeze and then changed again to northerlies. The second peak corresponds to the mid-evening surge (marked II). The passage of the sea-breeze and the mid-evening surge are both accompanied by an increase in wind speed, just like in the 8 October event. The mechanism for the increase in wind speed in this event is the same as for the 8 October event (figure not shown here). This mechanism is described later. The AWS data show a third period of marked moisture increase around 1830 CST, which is not reproduced by the model. We assume that the mechanism leading to the occurrence of this peak is the

Fig. 5 Comparison of time series of AWS data at Darwin on 14 and 15 October with model predictions: (a) 2 m water vapour mixing ratio, (b) 10-minute averaged 10 m wind direction, (c) 2 m temperature and (d) 10-minute averaged 10 m wind speed. Black lines correspond to the observations and red lines correspond to the model results. The Roman numbers correspond to events described in the text.

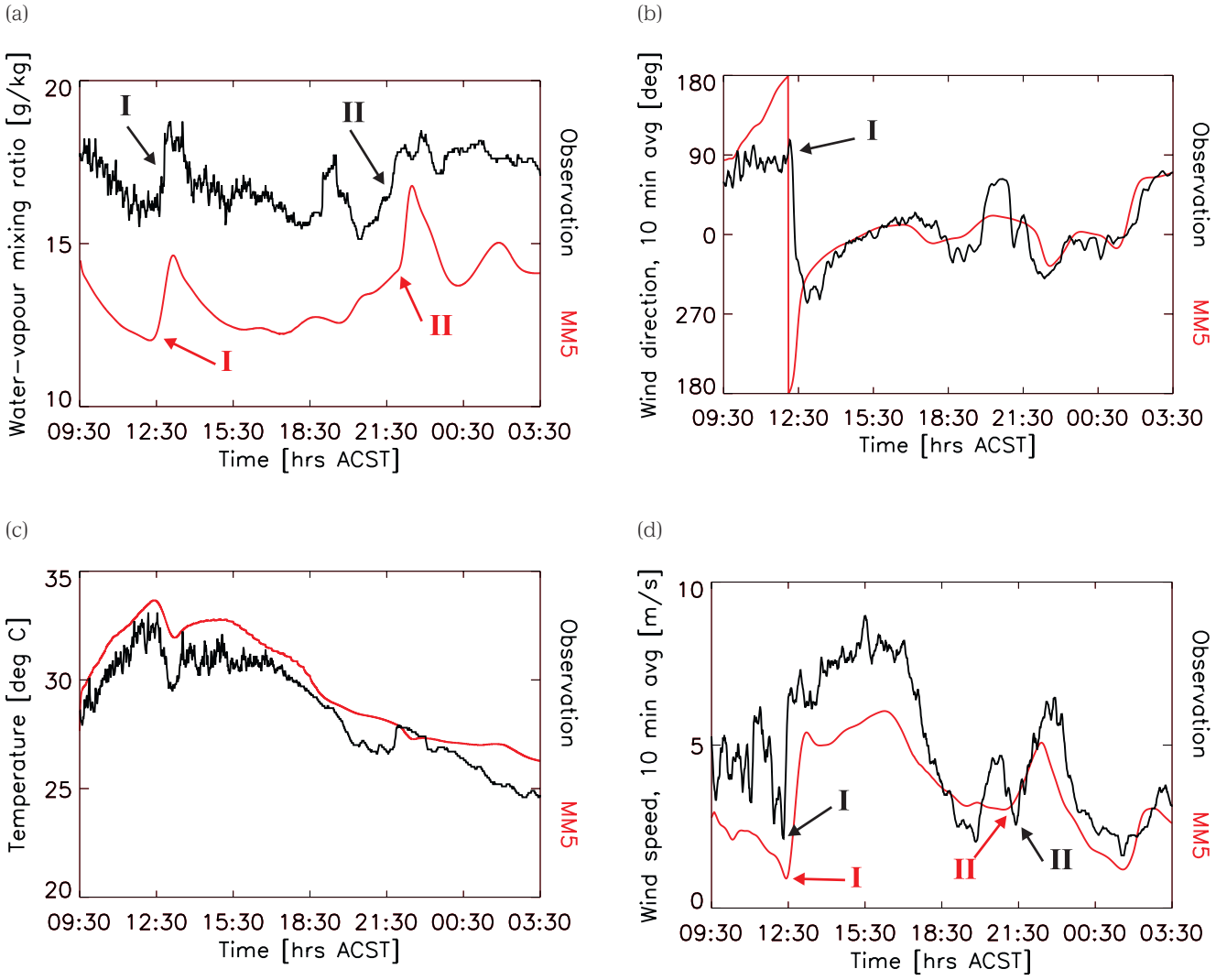

same as described earlier. Evidently, the occurrence of this moistening does not interfere with the mid-evening surge, as the model produces the mid-evening surge without having produced the late-afternoon moisture increase.

We return our attention now to the mid-evening surge and describe the course of events. Figure 6 shows the 2 m water vapour mixing ratio and the winds on the σ=0.955 surface in the model. By 1400 CST the easterly winds have advected dry inland air over Van Diemen Gulf. At this time, the regular sea-breeze had already reached the Darwin AWS. Northerly winds have then advected the southwestern edge of the dry band over Darwin. The dry air wedge has been transported further to the southwest by 1800 CST and its central part has passed over Darwin by 2200 CST. The subsequent humid air behind the wedge of dry air brings a humidity jump corresponding to a mid-evening surge.

Figure 7 shows a visible satellite image at 1603 CST on 14 October. The position of the sea-breeze fronts is presumably close to the edge of the cumulus cloud field, as in the event described previously. The image contrast between the band of dry air and the moist air behind the sea-breeze fronts is not as good as seen in the previous event, as there is little shallow convection on this day. The band of dry air is indicated by a dashed ellipse. The position of the dry air is estimated to be where the image is darkest, indicating a low reflectivity of the atmosphere. The position of the dry air in the model at 1600 CST (not shown here) corresponds very well with the position in the satellite image.

Fig. 6 Water vapour mixing ratio at 2 m (shaded) and horizontal wind vectors on the σ = 0.955 surface at (a) 1400 CST, (b) 1800 CST, (c) 2200 CST on 14 October and (d) 0200 CST on 15 October. The location of Darwin is indicated in all panels. The area shown in panels (b-d) is indicated by the box in panel (a).

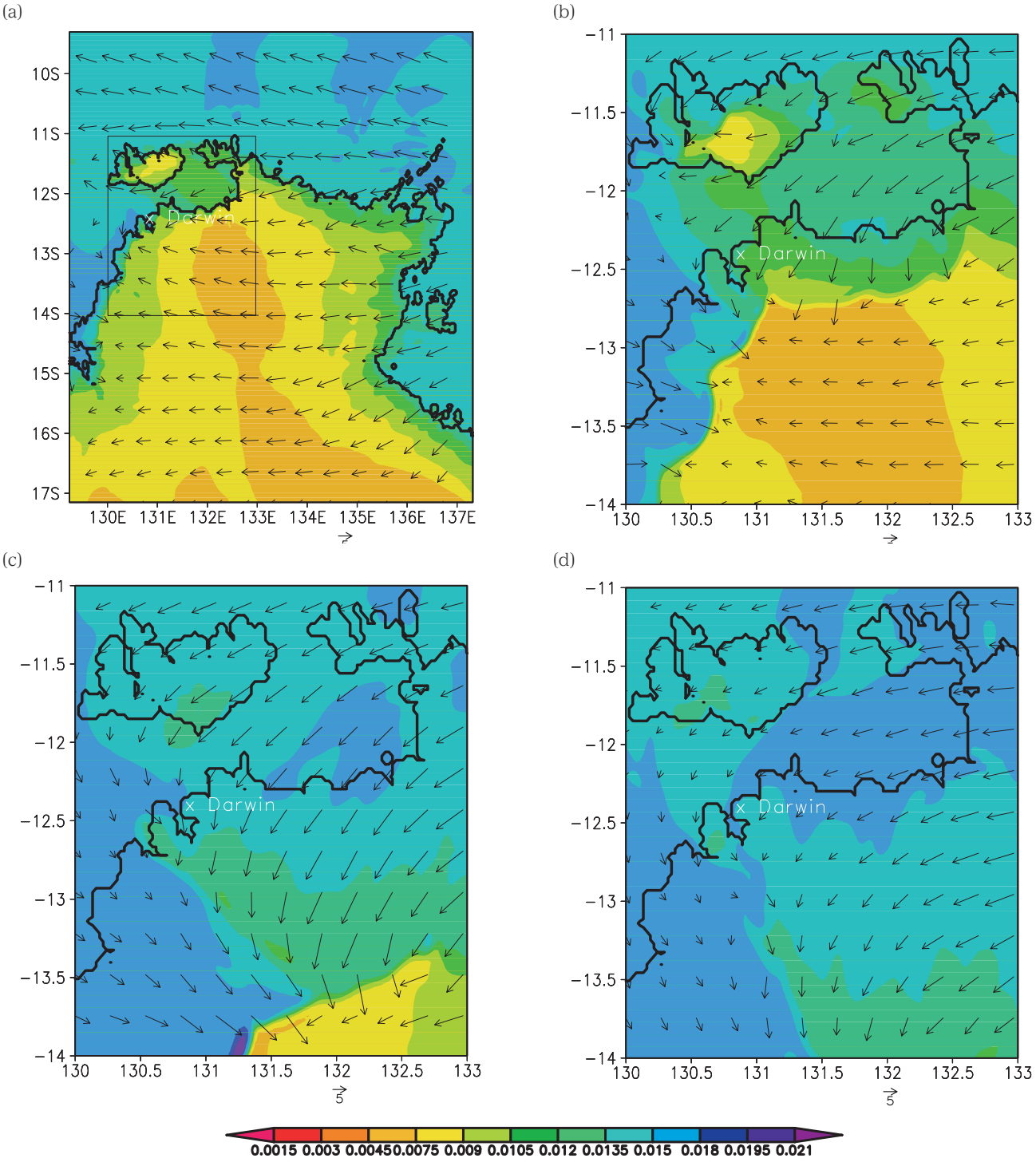

The null case of 5 November

Figure 8 shows the water vapour mixing ratio for the null case of 5 November. On this day, no mid-evening surge was observed and the model did not produce a signature that could be interpreted as one. Neither satellite images nor model results indicate that there was a dry band passing over Darwin from a northeasterly direction, as in the mid-evening surge events. The reason why there was no mid-evening surge on this day is explained in the following section.

Fig. 7 Meteosat visible image at 1603 CST, 14 October 2006.

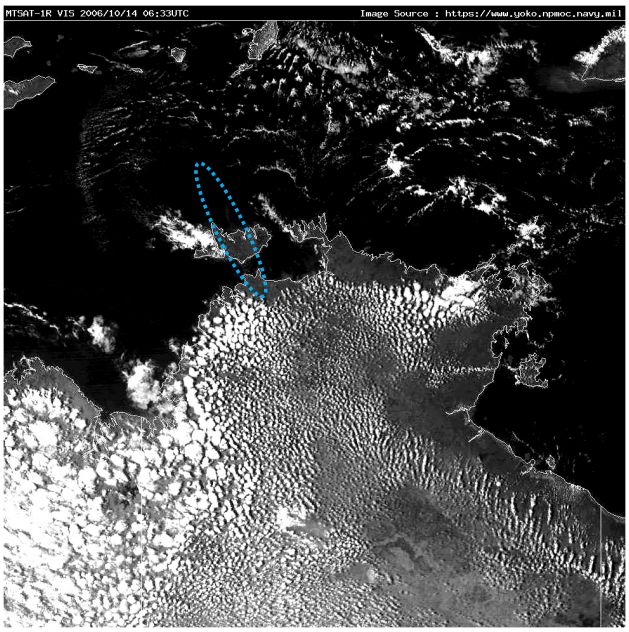

Fig. 8 Water-vapour mixing ratio at 2 m at Darwin on 5 November.

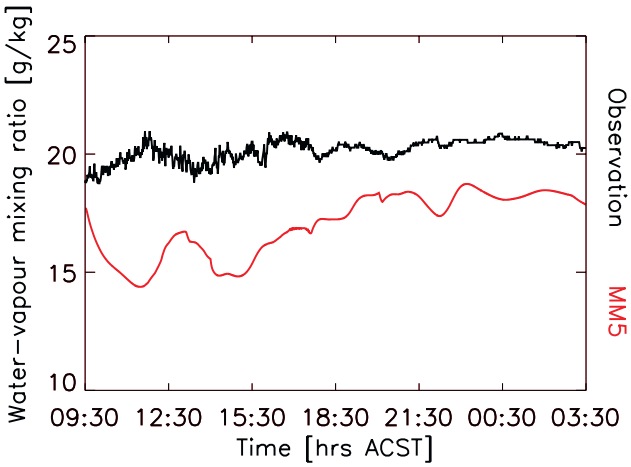

Favourable conditions for mid-evening surges

In order to provide forecasters with a rule of thumb to predict mid-evening surges on a daily basis, we analysed a wide range of ECMWF analysis charts for late 2006, paying particular attention to relative humidity charts at 0000 UTC and 1000 hPa with superimposed wind vectors at 925 hPa. Three noteworthy examples are shown in Fig. 9. It seems that there are two necessary conditions for mid-evening surges:

- The air over the Top End must be sufficiently dry, i.e. the 1000 hPa relative humidity should be below 50 per cent and extend northwards to at least 13°S. The drier the air is over the Top End, the stronger is the moisture contrast which is brought about by the mid-evening surge.
- The location of the dry air mass in relation to Darwin at 0000 UTC as well as the strength of the easterly winds at 950 hPa have to be favourable. These two factors determine the arrival time of the mid-evening surge. If the easterly winds are too strong (i.e. greater than about 10 m s^{-1}) and the western boundary of the dry air is too far west (around 132°W), the surge arrives during the day. The condition for a daytime surge will be satisfied also when the western boundary of the dry air is further to the east and the wind speed is correspondingly greater. On the other hand, if the easterly winds are too weak, for example less than 5 m s^{-1}, the dry air will not be advected over Darwin and no mid-evening surge will occur.

Figure 9(a) shows an example (the 8 October case described previously) in which these two conditions are satisfied (they are satisfied in all mid-evening surge events we analysed). The dry air over the Top End is located approximately between 133°E and 136°E. Figure 9(b) corresponds to our null case, 5 November (see Fig. 8). Top End air was too moist and there was no mid-evening surge in this example. Figure 9(c) shows an example in which the dry air extends far to the west (around 131°E). A surge was recorded in the afternoon on this day and could have been interpreted as the regular sea-breeze.

Idealised experiments

Here we describe two idealised experiments to underpin the foregoing results. Each of these calculations is initialised with a uniform easterly flow, one with a speed of 5 m s^{-1} and the other with a speed of 10 m s^{-1}. The soundings from Darwin, Weipa and Mt Isa are used to initialise the thermodynamic structure in these experiments. The Mount Isa sounding is used to represent the moisture profile of inland air south of 14.5°S and between 132°E and 134.5°E north of 14.5°S. The Darwin sounding is used for the moisture profile over land in coastal regions north of 14.5°S, both east of 134.5°E and west of 132°E. The Weipa sounding is used for the moisture profile over areas of sea. For simplicity, the temperature profile is taken to be an average of that in the three soundings. The model produces a mid-evening surge in both experiments. However, the results with the 10 m s^{-1} easterly flow are a little less realistic than with the 5 m s^{-1} background flow. A background wind speed of 10 m s^{-1} across the Top End is a little too strong to allow a sea-breeze to move inland from the west coast. With a background wind speed of 5 m s^{-1}, a sea-breeze flow moves inland from the west coast and a suitable flow configuration for producing a mid-evening surge becomes established over the Top End.

Figure 10(a) shows the water vapour mixing ratio and the wind field in the lowest model layer in the experiment with

Fig. 9 ECMWF analysis of relative humidity (shaded) at 1000 hPa and wind speed (black arrows) at 925 hPa and at 0000 UTC on (a) 8 October, (b) 5 November and (c) 4 October.

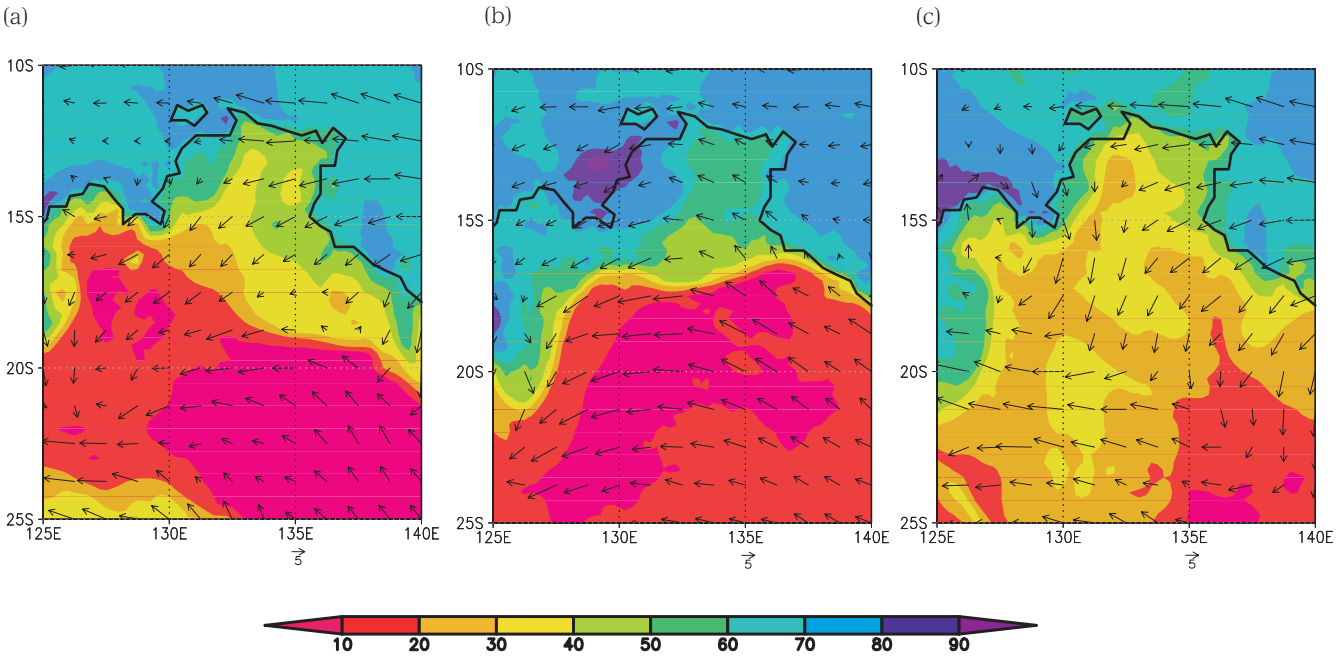

Fig. 10 Water vapour mixing ratio at 2 m (shaded) and horizontal wind vectors on the $\sigma = 0.955$ surface at (a) 0930 CST and (b) 2200 CST in the idealised experiment with 5 m s^{-1} background easterly flow. The location of Darwin is indicated in all panels.

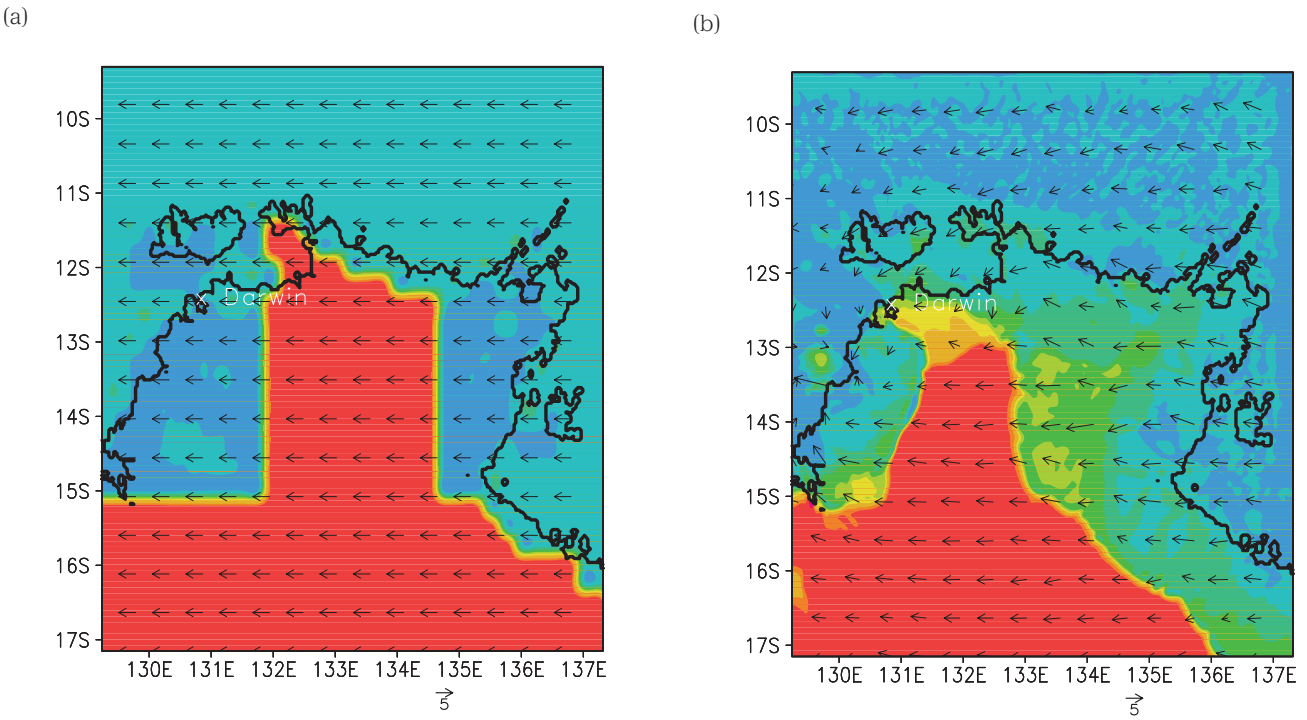

a 5 m s^{-1} background easterly wind flow. Figure 10(b) shows the same fields at 2200 CST. Compared to the observed cases, a quite realistic flow configuration has developed by this time and a dry band is just passing over Darwin. Figure 11 shows time series of the water vapour mixing ratio and 10 min averaged wind direction at Darwin in the idealised experiment and on 8 October for comparison. Apart from the absence of a late-afternoon moistening, the moisture profile shows the main observed features. After the sea-breeze circulation has become established, the wind directions are remarkably close to the wind direction in the observed case.

Fig. 11 Comparison of time series of AWS data at Darwin on 8 and 9 October with predictions from an idealised experiment with a 5 m s^{-1} background easterly flow: (a) 2 m water vapour mixing ratio, (b) 10-minute averaged 10 m wind direction.

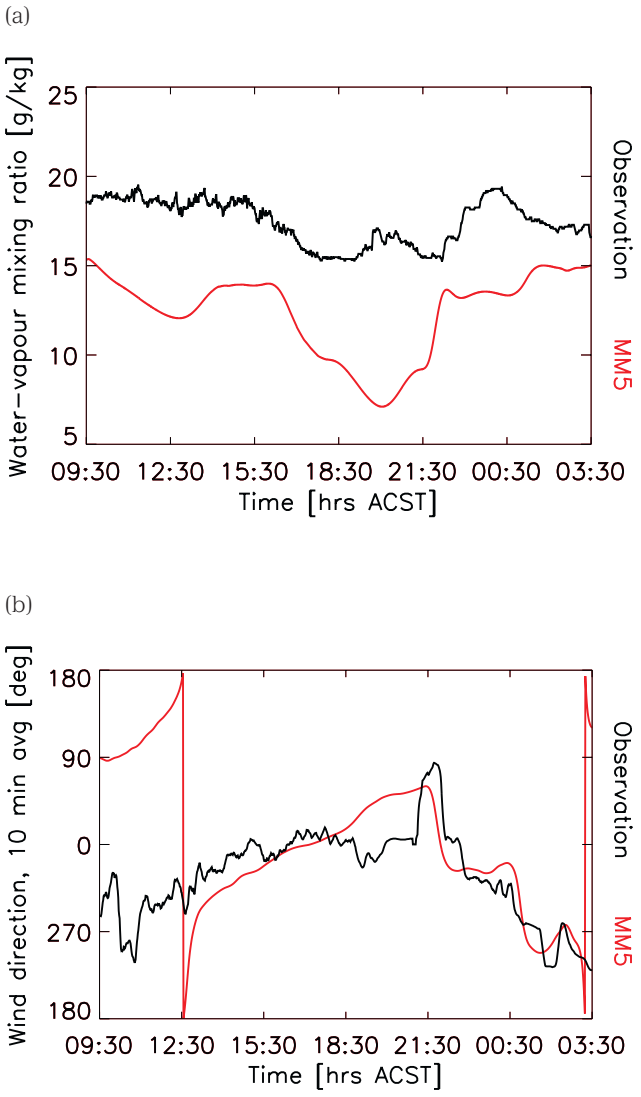

We refer now to the change in wind speed and direction accompanying the passage of the mid-evening surge. This passage coincides with the passage of a convergence zone between two different air masses. Figure 12(a) shows a 200 km long distance-height cross-section of water vapour mixing ratio and virtual potential temperature, θ_v, through the dry wedge (located around 40 km) at 2200 CST on 8 October. This event is described in detail in an earlier section. Values of θ_v associated with the dry tongue and the air south of it are slightly higher (approximately by 0.5 K in the dry band and 1 K 30 km south of it) than in the moist air to the northeast, indicating that the air in the dry tongue is slightly less dense. There is an elevated region of convergence, indicated by the thick solid lines in Fig. 12(a), along the leading edge of the moist air to the northeast.

Fig. 12 Distance-height cross section of virtual potential temperature (θ_v), water vapour mixing ratio from 13°S, 131°E to 11.5°S, 132°E and from 0 to 2000 m height above mean sea level at 2200 CST, 8 October 2006 (panel (a)) and in the idealised experiment with 5 m s^{-1} background wind speed (panel (b)). The location of the cross-section is indicated in Fig. 3(e). Water vapour mixing ratio is shaded and the dotted contours show θ_v up to 304 K (panel (a)) and up to 306 K (panel (b)). The thick solid and dashed contours show regions of strong (greater than $10^{-4} s^{-1}$ in magnitude) divergence and convergence, respectively.

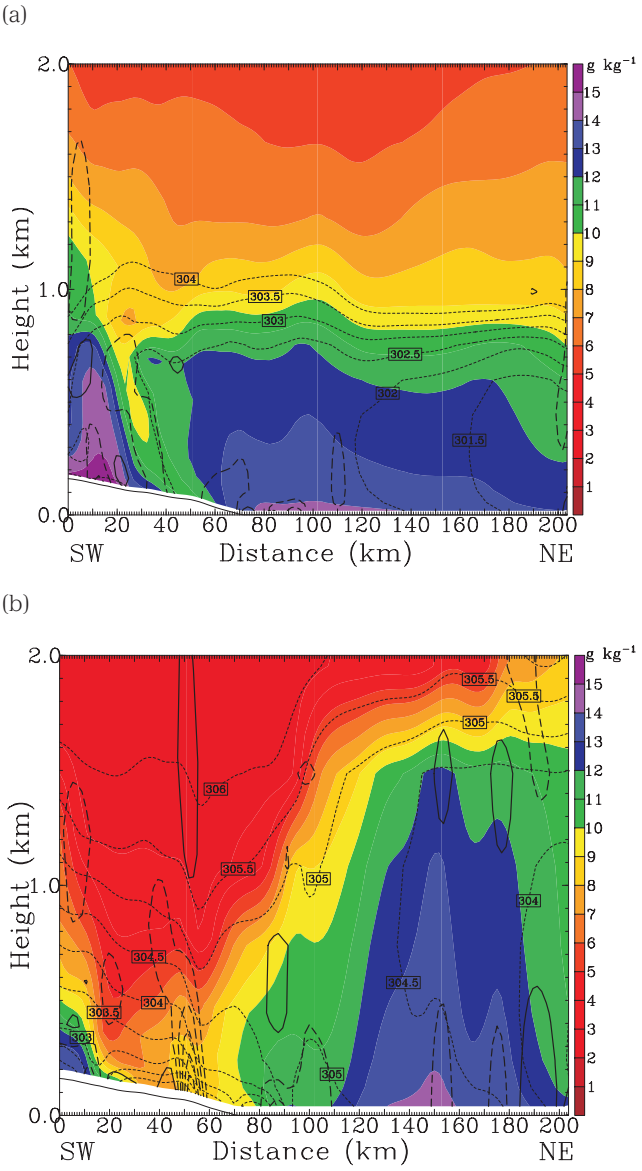

Figure 12(b) shows the situation at the same time for the idealised experiment with a 5 m s^{-1} background easterly flow. The dry wedge is evident also in this experiment and extends approximately from 20 km to 50 km, but it is drier than in the 8 October case. However, unlike the 8 October case, the moist maritime air to the northeast is slightly less dense (θ_v is about 0.5 to 1 K higher at the lowest few hundred

metres) than in the dry wedge. Significantly, there is again convergence between the two air masses at around 50 km, but the slightly lighter air runs into the denser air in this experiment. The common feature of the two calculations is the convergence zone between the dry wedge and the moist air to its northeast, whereas the temperature difference between the two air masses is different. These facts support our interpretation of the evening disturbance as a wind surge rather than a second sea-breeze.

Discussion and conclusions

The numerical model MM5 in the chosen configuration was able to reproduce mid-evening surges in all the six cases of our study. It did not capture the sudden increase in humidity during the daytime in one of the cases. We attribute this deficiency to slightly lower easterly wind speeds than observed. However, this feature does not apparently affect the model's ability to predict the mid-evening surge. The calculations indicate that the easterly winds advect dry inland air towards the Tiwi Islands. Subsequently, this band of dry air moves to the southwest towards Darwin and is followed by moist maritime air. Typically, the band of dry air passes over Darwin in the late evening and is followed by moister sea air. The arrival of the moist air is what was previously interpreted as a 'second sea-breeze'. We argue that a more appropriate term for this occurrence is a mid-evening surge because there is no appreciable horizontal gradient of virtual potential temperature (the temperature rise observed near the surface is most likely to be associated with the downward mixing of warm air as the wind freshens).

In a calculation for a null case, when no mid-evening surge was observed, the model did not produce a dry band.

We have found two favourable conditions for the occurrence of mid-evening surges, namely: the air over the Top End must be sufficiently dry and the strength of the broadscale easterlies combined with the position of the dry air at 0000 UTC must be suitable.

The good agreement between our idealised experiments and observations further strengthens our explanation for the occurrence and essence of the mid-evening surge.

Acknowledgments

We thank Sam Cleland and James Turnbull from the Bureau of Meteorology's Regional Forecasting Centre in Darwin. Sam drew our attention to the 'second sea-breeze' phenomenon and James kindly provided the relevant station data. We are grateful to the ECMWF for providing analysis data. Financial support for this study was provided by the German Research Council (Deutsche Forschungsgemeinschaft).

References

Dudhia, J. 1989. Numerical study of convection observed during the winter monsoon experiment using a mesoscale two-dimensional model. *J. Atmos. Sci., 46*, 3077-107.

Grell, G.A. 1993. Prognostic evaluation of assumptions used by cumulus parameterizations. *Mon. Weath. Rev., 121*, 764-87.

Grell, G.A., Dudhia, J. and Stauffer, D. 1995. A description of the 5th generation Penn State/NCAR mesoscale model (MM5). *Tech. Rep., 398*, NCAR, 122 pp.

Hong, S.-Y. and Pan, H.-L. 1996. Nonlocal boundary layer vertical diffusion in a medium-range forecast model. *Mon. Weath. Rev., 124*, 2322-39.

Smith, R.K., Reeder, M.J., Tapper, N.J. and Christie, D.R. 1995. Central Australian cold fronts. *Mon. Weath. Rev., 123*, 16-38.

Thomsen, G.L. 2006. Numerical simulations of low-level convergence lines over north-eastern Australia. PhD thesis, Meteorological Institute Munich, Theresienstr. 37, 80333 Munich, Germany. http://edoc.ub.uni-muenchen.de/archive/00005691/01/Thomsen_Gerald.pdf.

Thomsen, G.L., Reeder, M.J. and Smith, R.K. 2009. The diurnal evolution of cold fronts in the Australian subtropics. *Q. Jl R. Met. Soc., 135*, 395-411

Thomsen, G.L. and Smith, R.K. 2006. Simulations of low-level convergence lines over northeastern Australia. *Q. Jl R. Met. Soc., 132*, 691-707.

Thomsen, G.L. and Smith, R.K. 2008. The importance of the boundary layer parameterization in the prediction of low-level convergence lines. *Mon. Weath. Rev., 136*, 2173-85.